

RESEARCH ARTICLE

Kinetic and structural insights into enzymatic mechanism of succinic semialdehyde dehydrogenase from *Cyanothece* sp. ATCC51142

Congcong Xie¹, Zhi-Min Li², Fumei Bai¹, Ziwei Hu¹, Wei Zhang¹, Zhimin Li^{1*}

1 College of Bioscience and Bioengineering, Jiangxi Key Laboratory for Conservation and Utilization of Fungal Resources, Jiangxi Agricultural University, Nanchang, Jiangxi, China, **2** College of Science, Jiangxi Agricultural University, Nanchang, Jiangxi, China

These authors contributed equally to this work.

* zhiminli@jxau.edu.cn



OPEN ACCESS

Citation: Xie C, Li Z-M, Bai F, Hu Z, Zhang W, Li Z (2020) Kinetic and structural insights into enzymatic mechanism of succinic semialdehyde dehydrogenase from *Cyanothece* sp. ATCC51142. PLoS ONE 15(9): e0239372. <https://doi.org/10.1371/journal.pone.0239372>

Editor: Concepción Gonzalez-Bello, Universidad de Santiago de Compostela, SPAIN

Received: April 23, 2020

Accepted: September 6, 2020

Published: September 23, 2020

Copyright: © 2020 Xie et al. This is an open access article distributed under the terms of the [Creative Commons Attribution License](https://creativecommons.org/licenses/by/4.0/), which permits unrestricted use, distribution, and reproduction in any medium, provided the original author and source are credited.

Data Availability Statement: All relevant data are within the paper and its Supporting Information files.

Funding: This work was partially supported by Natural Science Foundation of Jiangxi Province (20161ACB21012) and National Natural Science Foundation of China (31860249). The funders had no role in study design, data collection and analysis, decision to publish, or preparation of the manuscript.

Abstract

As a ubiquitous enzyme, succinic semialdehyde dehydrogenase contributes significantly in many pathways including the tricarboxylic acid cycle and other metabolic processes such as detoxifying the accumulated succinic semialdehyde and surviving in nutrient-limiting conditions. Here the *cce4228* gene encoding succinic semialdehyde dehydrogenase from *Cyanothece* sp. ATCC51142 was cloned and the homogenous recombinant *cce4228* protein was obtained by Ni-NTA affinity chromatography. Biochemical characterization revealed that *cce4228* protein displayed optimal activity at presence of metal ions in basic condition. Although the binding affinity of *cce4228* protein with NAD⁺ was about 50-fold lower than that of *cce4228* with NADP⁺, the catalytic efficiency of *cce4228* protein towards succinic semialdehyde with saturated concentration of NADP⁺ is same as that with saturated concentration of NAD⁺ as its cofactors. Meanwhile, the catalytic activity of *cce4228* was competitively inhibited by succinic semialdehyde substrate. Kinetic and structural analysis demonstrated that the conserved Cys262 and Glu228 residues were crucial for the catalytic activity of *cce4228* protein and the Ser157 and Lys154 residues were determinants of cofactor preference.

Introduction

Cyanobacteria are a kind of ancient prokaryotes which carry out oxygenic photosynthesis to change atmospheric chemistry and play an important role in aquatic ecosystems [1]. There are more than 2000 species in 150 genera of cyanobacteria with various shapes and sizes around the world [2]. *Cyanothece* sp. ATCC51142, one species of the genus *Cyanothece*, is the first genome sequenced diazotroph that can fix atmospheric nitrogen [3]. Cyanobacteria become attractive due to its capability of being genetically engineered to produce biofuels and other value-added products [4]. In addition, potent N₂-fixing cyanobacteria are exploited as biofactory to produce feedstocks in the field of agriculture [5].

Competing interests: The authors have declared that no competing interests exist.

In canonical tricarboxylic acid (TCA) cycle, α -ketoglutarate (α -KG) is transformed into succinic acid through succinyl-CoA intermediate by two functional enzymes of α -KG dehydrogenase and succinyl-CoA synthetase. Unlike the canonical TCA cycle, α -KG is catalyzed by α -KG decarboxylase to generate succinic semialdehyde (SSA), which then is catalyzed by succinic semialdehyde dehydrogenase (SSADH) to produce succinic acid in many cyanobacteria because of the absence of key α -KG dehydrogenase [6, 7]. BLAST sequence analysis showed that the two genes of *cce4227* and *cce4228* encoded respective α -KG decarboxylase and SSADH in *Cyanothece* sp. ATCC51142. However, there is no detailed physiological and biochemical characterization of *cce4227* and *cce4228* proteins.

SSADH (EC 1.2.1.79) was an NAD(P)⁺-dependent oxidoreductase, one member of the aldehyde dehydrogenase superfamily. The oxidation of SSA was catalyzed by SSADH with NAD(P)⁺ as the cofactor to produce succinic acid, which is an intermediate in the TCA cycle. Therefore, SSADH played a vital role in metabolic pathways such as α -ketoglutarate shunt [8, 9], γ -aminobutyric (GABA) shunt [7, 10] and *p*-hydroxyphenylacetate shunt [11]. Once SSADH was missing in these TCA cycle variations, toxic substrates such as SSA, GABA and 4-hydroxybutyric acid (GHB) would accumulate in large quantities in cells, which could cause different degrees of harm in different organisms. In human, SSADH deficiency would lead to a rare hereditary neuropharmacological disorder, which was displayed by the clinical phenotype such as psychomotor arrest, developmental delay, language impairment, ataxia, lethargy and convulsion [12–14]. SSADH deficiency not only causes changes of development and phenotype in plants, but also makes plants sensitive to heat and UV radiation caused by the reactive oxygen intermediate [15, 16]. For bacteria, SSADH deficiency would lead to an imbalance of carbon and nitrogen metabolism in cells [17]. In addition, SSADH could promote the antioxidant defense ability of mitochondria by 4-hydroxynonenal which was the final product of oxidative peroxide lipid degradation [18].

Other than the physiological functional study of SSADH *in vivo*, there were many studies on its catalytic function and cofactor preference in recent years [19–22]. NADP⁺ or NAD⁺ was required as a hydride acceptor in the reaction of SSA to succinic acid catalyzed by SSADH. Initially, two genes of *YneI* and *GabD* were found in *Escherichia coli* to encode two types of SSADHs, which were dependent on NAD(P)⁺ and NADP⁺ cofactors, respectively [23]. As a result, SSADHs were categorized to two classes of *YneI* and *GabD* on account of cofactor preference. Generally, SSADHs with a small Ser residue in the active site preferred NADP⁺ cofactor since its active site could adapt the adenosine nucleoside phosphate group in NADP⁺ cofactor. SSADHs from *Streptococcus pyogenes* [24] and *Anabaena* sp. PCC7120 [25] were examples. On the other hand, SSADH from *Salmonella typhimurium* preferred NAD⁺ cofactor because its active center had a larger Lys160 residue [22], which could not accommodate the adenosine nucleoside phosphate group.

In this study, the detailed kinetic characterization and homology modeling of *cce4228* protein from *Cyanothece* sp. ATCC51142 were carried out. Biochemical characterization revealed that *cce4228* protein displayed optimal activity with MgCl₂ at basic condition. Moreover, *cce4228* protein showed same catalytic efficiency with saturated concentration of NADP⁺ or NAD⁺ as cofactor, although *cce4228* protein had a higher binding affinity for NADP⁺ than NAD⁺. Site-directed mutagenesis demonstrated that the conserved Cys262 and Glu228 residues were critical for the enzymatic activity of *cce4228* protein. Homology modeling revealed the structural basis of Ser157 and Lys154 residues to determine cofactor preference.

Materials and methods

Chemicals and reagents

E. coli TransDH5 α and BL21(DE3) competent cells, pET-28a vector were prepared and preserved by our lab. The genomic DNA of *Cyanothece* sp. ATCC51142 was purchased from

American Type Culture Collection. DNA polymerase, DNA marker, *Nde*I and *Xho*I endonucleases, Fast Mutagenesis Kit were obtained from TransGen Biotech (Beijing, China). T4 DNA ligase, 2×Premix Taq and *Dpn*I were products of TaKaRa Biotechnology (Dalian, China).

Overexpression and purification of *cce4228* protein

Open reading frame of *cce4228* gene from *Cyanotheca* sp. ATCC51142 (GenBank: ACB53576), encoding a succinic semialdehyde dehydrogenase, was amplified from the template of genomic DNA of *Cyanotheca* sp. ATCC51142 with commercial primers (S1 Table in [S1 File](#)) by PCR. The constructed recombinant pET28a-*cce4228* plasmid was transformed into *TransDH5α* competent cells and verified by DNA sequencing. Recombinant *cce4228* protein with 6xHis at N-terminus was obtained as described previously [26]. Briefly, pET28a-*cce4228* plasmid transformed *E. coli* BL21(DE3) cells were grown at 25°C, 220 rpm in Luria broth (LB) media with 50 μg/mL kanamycin, then the cells were induced by 0.2 mM isopropyl-β-D-thiogalactopyranoside when OD_{600nm} of cells reached 0.8 and cultured for another 24 h at 25°C, 180 rpm. The cells were centrifuged and then lysed by sonication. Recombinant *cce4228* protein were purified to be homogenous with Ni-NTA agarose resin and dialysis in 50 mM Tris-HCl, pH 8.0 was used to remove imidazole from the protein preparation. Mutants of *cce4228* protein were obtained by performing the same protocol as the wild-type except that mutations in pET28a-*cce4228* plasmid were introduced by site-directed mutagenesis with commercial primers (S1 Table in [S1 File](#)) according to the reference [25].

Catalytic activity determination of *cce4228* protein

The catalytic activity of *cce4228* protein was determined according to the procedures described in reference [25]. Briefly, specific amounts of NADP⁺, MgCl₂ and purified *cce4228* protein were incubated in 50 mM 2-(*N*-cyclohexylamino) ethanesulfonic acid (CHES), pH 9.0 buffer for 5 min at 25°C, and then various concentrations of SSA were added to the assay solution to start the reaction. Absorbance of reaction mixture at 340 nm was recorded to calculate reaction initial velocity. The obtained initial reaction velocities and concentrations of SSA substrate were fitted with the following equations by KaleidaGraph Software to obtain kinetic parameters. All measurements were repeated three times.

$$v = v_{\max}[S]/([S] + Km), \text{ without inhibitor} \quad (1)$$

$$v = v_{\max}/(1 + K_m/[S] + [S]/K_i), \text{ excess - substrate inhibition} \quad (2)$$

Where v was the calculated initial velocity, $[S]$ was the concentration of substrate. v_{\max} , K_m and K_i , indicating respective maximum reaction velocity, Michaelis-Menten constant and inhibitory constant of the substrate, were given by the software. The error bars indicated the standard errors of the mean (SEM) in this study.

Effects of chemical reagents on the activity of *cce4228* wild-type

The effects of MgCl₂, ethylene diamine tetraacetic acid (EDTA), dithiothreitol (DTT) and β-mercaptoethanol (β-ME) on the catalytic activity of wild-type *cce4228* protein were investigated by measuring the reaction initial velocities at presence of the above chemicals (2 mM) in reaction solution.

Structure prediction and homology modeling for *cce4228*

The amino acid sequence of *cce4228* protein and SSADHs from other sources were aligned using CluslalW method in MEGA 6.0 software. The tertiary structure of *cce4228* protein was simulated with the ternary complex of SSADH from *Synechococcus* sp. PCC7002 with NADP⁺ and SSA (PDB ID: 3VZ3) as template by Swiss-Model [27] and depicted by Pymol 1.503 software [28]. The SSADH protein in 3VZ3 is that of the non-catalytic Cys262Ala variant [19]. The online SAVES v5.0 server (<https://servicesn.mbi.ucla.edu/SAVES/>) was used to evaluate the quality of simulated three-dimensional structure of *cce4228* protein.

Results and discussion

Purification and mass determination of recombinant SSADH

Open reading frame of *cce4228* gene encoding SSADH was cloned from the genomic DNA of *Cyanothece* sp. ATCC51142 successfully, and recombinant wild-type *cce4228* protein was induced and overexpressed in *E. coli* BL21(DE3) [26]. After that, recombinant *cce4228* protein was purified by fast protein liquid chromatography with Ni-NTA resin. The yield of homogenous *cce4228* wild-type protein was 15 mg/g wet cells. SDS-PAGE estimated the approximate subunit molecular mass of *cce4228* protein to be 50 kDa (Fig 1), which is close to the theoretical subunit mass of *cce4228* protein with N-terminal 6xHis-tag (52518.13 Da). Meanwhile, the native mass of *cce4228* protein was calculated to be *ca.* 109 kDa by size exclusion chromatography with standard protein ladders (S1 Fig in S1 File), which indicated that *cce4228* protein was most probably a dimer. The oligomeric status of recombinant *cce4228* protein was the same as that of SSADHs from *Synechococcus* sp. PCC7002 and *Anabaena* sp. PCC7120 [19, 20, 25]. The mutants of *cce4228* protein were overexpressed and purified to be homogenous with close yield and purity as that of wide-type *cce4228* (Fig 1).

The effects of chemical reagents on catalytic activity of *cce4228* wild-type

Previous results revealed that the catalytic activity of *cce4228* protein would be either increased or decreased after adding metal ions into activity assay solution [26]. In this study, the activity of wild-type *cce4228* protein would be decreased by 2-fold with the addition of 2 mM EDTA to remove the rudimental metal ions in assay buffer (the first bar vs the second bar) (Fig 2).

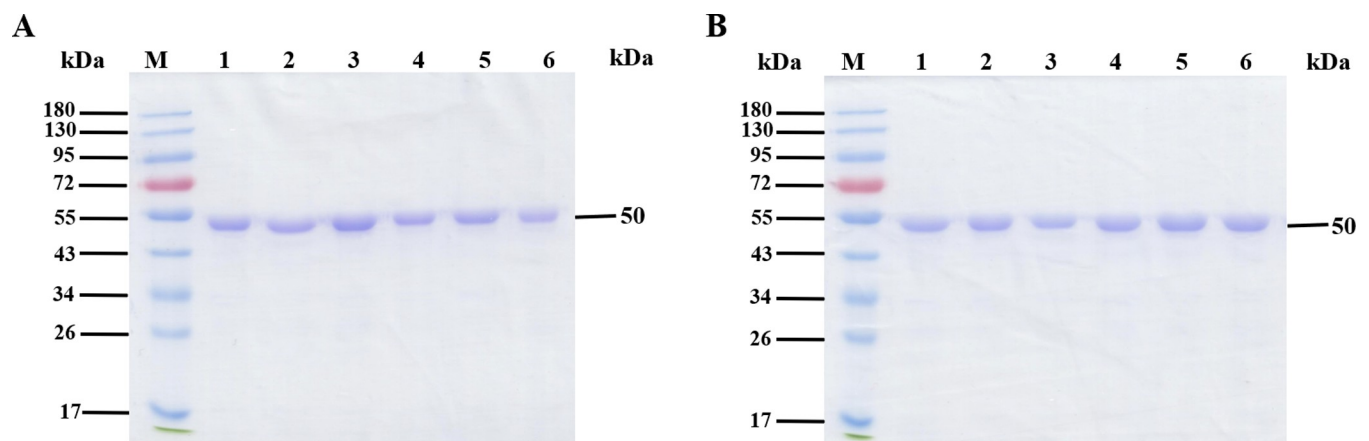


Fig 1. Purification of *cce4228* wild-type and mutants. A. Lane M: protein marker; Lane 1–6: wild-type, Cys262Ala, Glu228Ala, Asn131Ala, Ser157Glu and Lys154Ala, respectively. B. Lane M: protein marker; Lane 1–6: Ser420Ala, Arg139Ala, Ser207Ala, Trp135Ala, Trp130Ala and Glu360Ala, respectively. 20 μ g protein was deposited for both gels.

<https://doi.org/10.1371/journal.pone.0239372.g001>

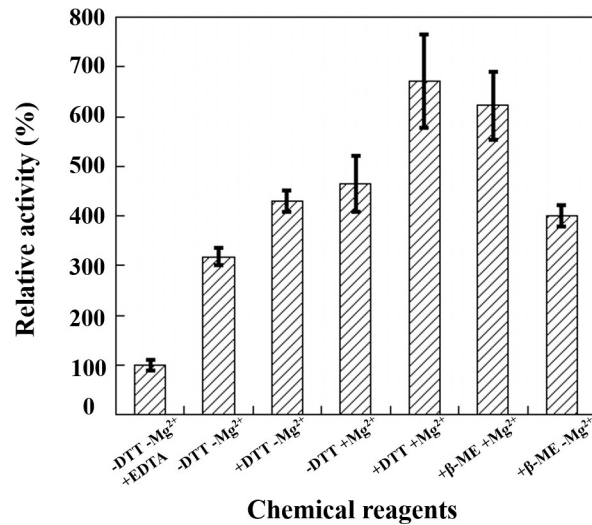


Fig 2. The effects of chemical reagents on catalytic activity of cce4228 wild-type protein. “+” indicates specific amounts of agents as indicated in the text were added to the assay solution, “-” indicates that agents not added to the assay solution. The catalytic initial velocity of cce4228 with 2 mM EDTA in assay solution was designated arbitrarily as 100% relative activity. The concentrations of cce4228 protein, SSA and NADP⁺ were fixed at 0.134 μM, 0.2 mM and 0.5 mM, respectively.

<https://doi.org/10.1371/journal.pone.0239372.g002>

This result indicated that the metal ion was important for cce4228 to display full function. As shown in Fig 2, the catalytic activity of cce4228 protein was elevated by 4~6 fold after adding 2 mM Mg²⁺ into assay buffer (the fourth, fifth or sixth bar vs the first bar). Meanwhile, the K_m value of Mg²⁺ and cce4228 protein was measured to be 6.24 μM [26], which could explain the low activity of cce4228 protein with 2 mM EDTA in the reaction solution. Since Cys residue in cce4228 protein was thought to function as a nucleophile in the catalytic mechanism, the reducing agent of DTT or β-ME was investigated whether it would affect the activity. The results showed that the reducing agents did not seem to have a considerable effect on the enzymatic activity of cce4228 protein in the optimal pH (the fifth or sixth bar vs the fourth bar in Fig 2). It indicated that the nucleophilic Cys residue was in the reduced state [29]. This indicative finding was confirmed by the fact that the Cys262 in the active site of cce4228 did not form a disulfide bond with other Cys residues, although there were six Cys residues in cce4228 protein (S2 Fig in S1 File).

Cofactor preference of cce4228 protein

The amino acid sequence analysis revealed that cce4228 protein had Ser157 and Lys154 residues in its active center which might determine the cofactor preference (S3 Fig in S1 File). Meanwhile, the results of enzymatic kinetic experiments showed that cce4228 protein could use either NAD⁺ or NADP⁺ as cofactor (Table 1). The K_m values of cofactors with cce4228 were 1.7 mM and 0.034 mM for NAD⁺ and NADP⁺, respectively. Obviously, the binding affinity of NAD⁺ and cce4228 protein was *ca.* 50-fold lower than that of NADP⁺ and cce4228 protein if the K_m values were used as an estimation of the K_d values. However, cce4228 showed similar catalytic efficiency towards SSA at saturated concentration of NAD⁺ or NADP⁺. The k_{cat}/K_m values of cce4228 wild-type were 487 mM⁻¹s⁻¹ and 435 mM⁻¹s⁻¹ with the cofactors of NADP⁺ and NAD⁺, respectively (Table 1). As a comparison, the catalytic efficiency of SSADH from *Anabaena* sp. PCC7120 towards SSA with NAD⁺ as cofactor was 8-fold lower than that with NADP⁺ as cofactor [25]. Furthermore, the kinetic pattern revealed that SSA substrate

Table 1. Kinetic parameters of cce4228 wild-type and mutants with different cofactors.

Cofactor	Parameters	wild-type ^e	Ser157Glu	Lys154Ala
NADP ⁺	K_m^{SSA} (mM) ^a	0.008 ± 0.003	0.0028 ± 0.0007	0.02 ± 0.01
	K_i^{SSA} (mM) ^a	0.8 ± 0.2	0.12 ± 0.02	0.02 ± 0.01
	k_{cat}^{SSA} (s ⁻¹) ^a	3.9 ± 0.3	1.5 ± 0.1	0.10 ± 0.05
	k_{cat}/K_m^{SSA} (mM ⁻¹ s ⁻¹) ^a	487	535	5
	KNADP+ m (mM) ^b	0.034 ± 0.002	1.1 ± 0.2	6.1 ± 1.5
NAD ⁺	K_m^{SSA} (mM) ^c	0.004 ± 0.001	0.003 ± 0.001	0.02 ± 0.01
	K_i^{SSA} (mM) ^c	0.052 ± 0.004	0.13 ± 0.03	0.02 ± 0.01
	k_{cat}^{SSA} (s ⁻¹) ^c	1.74 ± 0.08	0.58 ± 0.05	0.13 ± 0.07
	k_{cat}/K_m^{SSA} (mM ⁻¹ s ⁻¹) ^c	435	193	6.5
	KNAD+ m (mM) ^d	1.7 ± 0.2	0.51 ± 0.04	1.5 ± 0.4

^a The concentrations of NADP⁺ were fixed at 0.5 mM, 10 mM and 8 mM for wild-type, Ser157Glu and Lys154Ala, respectively;

^b The concentrations of SSA were fixed at 0.2 mM, 0.02 mM and 0.02 mM for wild-type, Ser157Glu and Lys154Ala, respectively;

^c The concentrations of NAD⁺ were fixed at 10 mM, 6 mM and 5 mM for wild-type, Ser157Glu and Lys154Ala, respectively;

^d The concentrations of SSA were fixed at 0.02 mM for all of wild-type, Ser157Glu and Lys154Ala;

^e data from ref. [26].

<https://doi.org/10.1371/journal.pone.0239372.t001>

would inhibit the catalytic activity of cce4228 [26]. When the concentrations of SSA were increased to 0.02 mM and 0.1 mM with NAD⁺ and NADP⁺ as respective cofactors, the reaction rate of cce4228 would start to decrease [26]. The calculated inhibition constant (K_i) values were 0.052 mM and 0.8 mM with NAD⁺ and NADP⁺ as cofactors, respectively (Table 1). Structural insight demonstrated that the SSA substrate inhibited the activity of SSADH from *Streptococcus pyogenes* by occupying the binding site of cofactor in the active center [30]. Actually, our kinetic results proved that SSA competitively inhibited the activity of cce4228 protein when NADP⁺ was used as cofactor (Fig 3). Since the binding affinity of NADP⁺ with cce4228 was 50-fold higher than that of NAD⁺ with cce4228, the inhibitive concentration of SSA to cce4228 wild-type was much higher with NADP⁺ as cofactor than that with NAD⁺ as cofactor. As a result, it looked like that NADP⁺ not NAD⁺ was the preferred cofactor for cce4228 wild-type protein.

It was reported that the Ser157 of SSADH from *Synechococcus* sp. PCC7002 and *Anabaena* sp. PCC7120 functioned as cofactor preference determinant [20, 25]. To identify the residues involved in cofactor selectivity of cce4228 protein, the partial amino acid sequences of SSADHs from different sources were aligned (S3 Fig in S1 File). As shown in S3 Fig in S1 File, the corresponding residues of Ser157 in cce4228 were Glu231 and Glu225 in respective human SSADH and aldehyde dehydrogenase from *Arabidopsis thaliana*, both of which utilized NAD⁺ as their cofactor. Therefore, the cce4228 Ser157Glu mutant was constructed and the cofactor preference of Ser157Glu was further explored. The K_m value of NADP⁺ with Ser157Glu was 1.1 mM, whereas the K_m value of NAD⁺ with Ser157Glu was 0.51 mM (Table 1 and S4 Fig in S1 File). Compared to the binding affinity of wild-type cce4228 with cofactors, the binding affinity of Ser157Glu with NADP⁺ decreased by 30-fold (0.034 mM vs 1.1 mM), whereas the binding affinity of Ser157Glu with NAD⁺ increased by 3-fold (1.7 mM vs 0.51 mM) (Table 1). Obviously, the Ser157 residue of cce4228 protein functioned as a determinant of cofactor preference. Previous study showed that Lys160 residue in the active center determined the cofactor preference of SSADH from *Salmonella typhimurium*, which utilized NAD⁺ as its preferred cofactor [22]. The corresponding residue of Lys160 of SSADH from *Salmonella typhimurium* in cce4228 protein was Lys154 (S3 Fig in S1 File). Therefore, the Lys154Ala mutant was

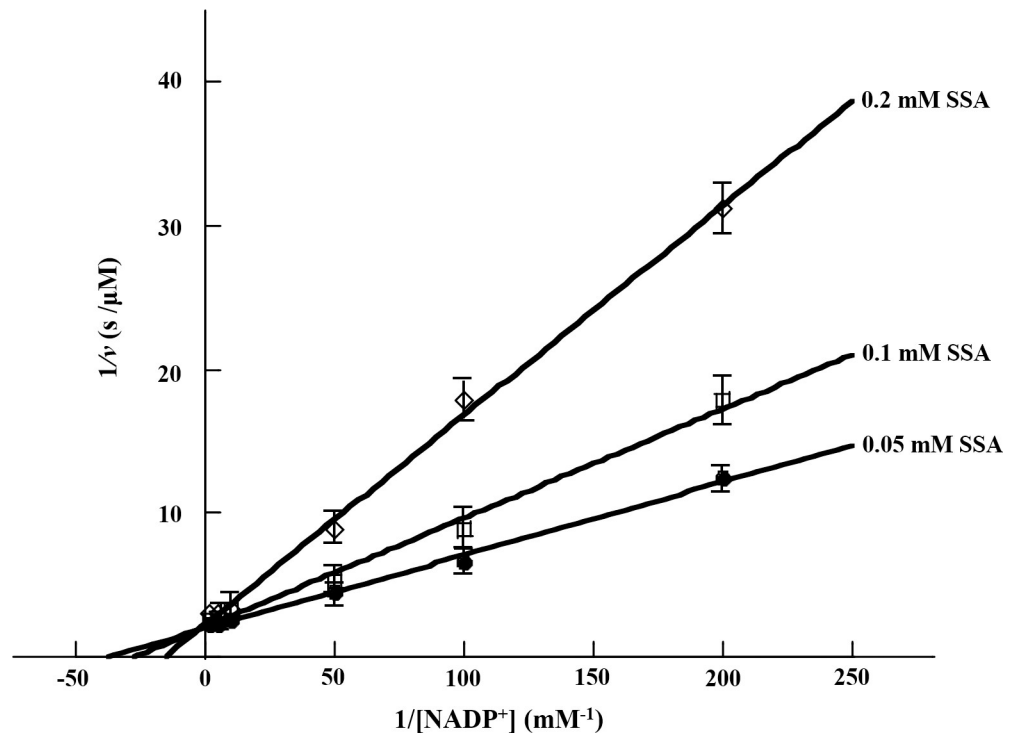


Fig 3. Lineweaver-Burk plot of *cce4228* wild-type protein with NADP^+ cofactor as substrate and SSA as inhibitor. The SSA concentrations were as labelled in the figure.

<https://doi.org/10.1371/journal.pone.0239372.g003>

constructed and its cofactor preference was further investigated. Expectedly, Lys154Ala mutant displayed cofactor preference to NAD^+ rather than NADP^+ . The K_m values of Lys154Ala with NAD^+ and NADP^+ were 1.5 mM and 6.1 mM, respectively (Table 1 and S5 Fig in S1 File). Interestingly, the binding affinity of *cce4228* wild-type protein with NADP^+ was much higher than that of Lys154Ala with NADP^+ (0.034 mM vs 6.1 mM). It was worth pointing out that the k_{cat} values of Lys154Ala decreased dramatically with either NAD^+ or NADP^+ as cofactor, compared to the corresponding values of *cce4228* wild-type, although the binding affinity of SSA with *cce4228* wild-type or mutants did not change substantially. As a result, the catalytic efficiency of Lys154Ala was decreased by 100-fold to $5 \text{ mM}^{-1}\text{s}^{-1}$ with NADP^+ as cofactor, compared to $487 \text{ mM}^{-1}\text{s}^{-1}$ for *cce4228* wild-type (Table 1). It was the same case for Lys154Ala with NAD^+ as cofactor (Table 1).

The steady-state kinetic assay of *cce4228* wild-type and mutants

To reveal the residues of *cce4228* protein responsible for its catalytic activity, several residues in the enzyme active center or allosteric site were mutated. The Cys residue near the SSA substrate was believed to function as a nucleophile to attack SSA or NAD(P)^+ as the first step in catalytic mechanism of SSADH [20, 30]. As a result, the *cce4228* Cys262Ala mutant showed no activity to SSA (Fig 4 and S2 Table in S1 File). Meanwhile, Glu228Ala mutation rendered *cce4228* inactive because the general base function by Glu228 vanished with this mutation. The Asn131Ala mutation would also inactivate *cce4228* (Fig 4 and S2 Table in S1 File). Although the k_{cat} of Ser420Ala increased by 2-fold, the K_m of Ser420Ala with *cce4228* increased by 9-fold. As a result, the catalytic efficiency (k_{cat}/K_m) of Ser420Ala was only 25% of that of *cce4228* wild-type overall (Fig 4, S6 Fig and S2 Table in S1 File). Arg139Ala mutant

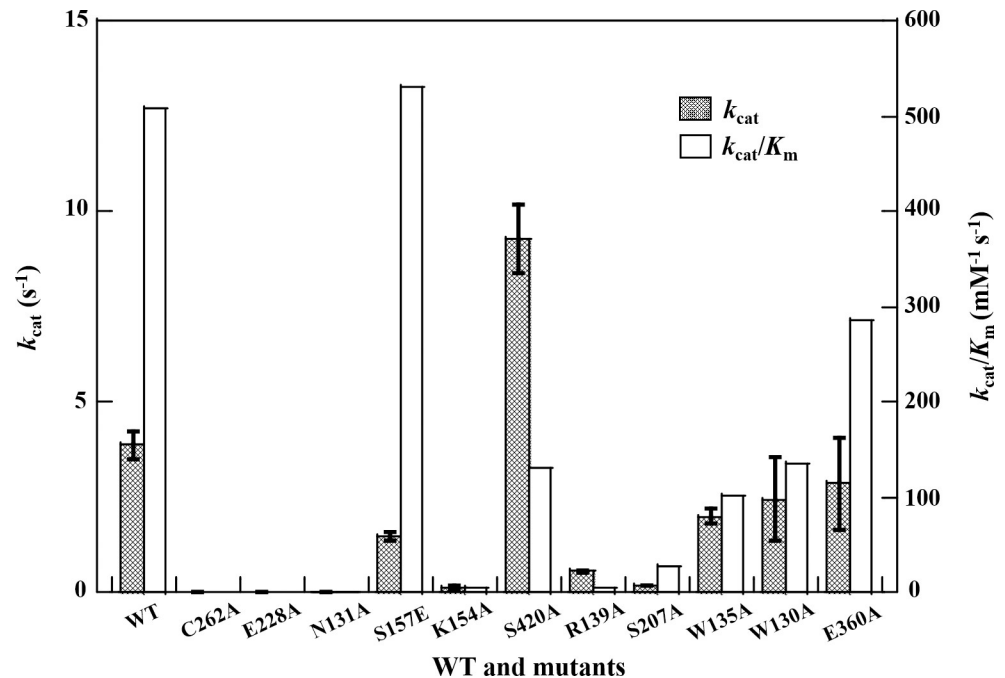


Fig 4. The k_{cat} and k_{cat}/K_m values of *cce4228* wild-type and mutants with $NADP^+$ as cofactor.

<https://doi.org/10.1371/journal.pone.0239372.g004>

showed substantially reduced binding affinity with SSA, whereas Ser207Ala had a similar binding affinity with SSA as that of *cce4228* wild-type (S2 Table and S6 Fig in S1 File). These results indicated that Ser420 and Arg139 residues played important role in stabilizing SSA substrate. In addition, the mutations at Trp135, Trp130 and Glu360 would slightly affect their binding affinity to SSA or $NADP^+$ (S2 Table and S6 Fig in S1 File). The catalytic efficiency of Trp135Ala, Trp130Ala and Glu360Ala reached 59%, 63% and 65% of that of *cce4228* wild-type protein, respectively (Fig 4 and S2 Table in S1 File). Since all the aforementioned residues located in either SSA substrate binding pocket or $NADP^+$ cofactor binding pocket, and the mutations at these residues would either affect the binding affinity or catalytic turnover rate, it was reasonable to conclude that there was synergistic effect between these residues in determining catalytic efficiency and cofactor preference.

Homology modeling of wild-type *cce4228* protein

Based on phylogenetic analysis of *cce4228* from *Cyanothece* sp. ATCC51142 with other SSADHs from different sources [26], we found that *cce4228* protein was closely related to a2771 from *Synechococcus* sp. PCC 7002, whose crystal structure was available [19, 20]. The amino acid sequence identities between *cce4228* and a2771 were 65% (Fig 5 and S7 Fig in S1 File). Therefore, the crystal structure of a2771 (PDB ID: 3VZ3) was used as template to construct the model structure of *cce4228* by Swiss-Model and the model cartoon structure of *cce4228* was displayed by Pymol 1.503 software. The model structure of *cce4228* was almost overlapped with a2771 protein due to the high homology between *cce4228* and a2771 (Fig 6). The Ramachandran plot showed that 93.6% of the residues of model structure of *cce4228* were in the most favored regions and only 0.3% of the residues were in the disallowed regions, which indicated that the model structure of *cce4228* was with great quality and high reliability (S8 Fig in S1 File). As shown in Fig 6B, the Ser157 and Lys154 residues of SSADH from *Synechococcus* sp. PCC 7002 were close to the adenosine nucleoside phosphate group of $NADP^+$.

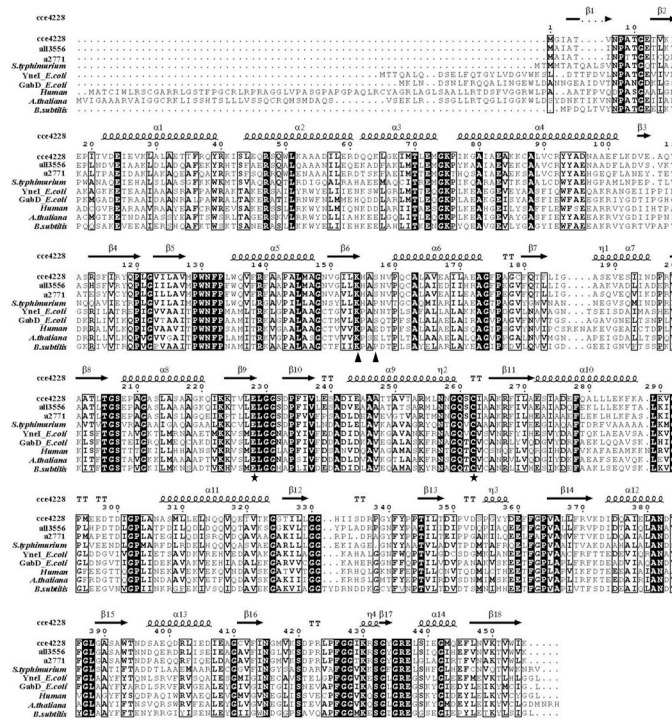


Fig 5. Amino acid sequence alignment of succinic semialdehyde dehydrogenases from different sources. SSADH sequences retrieved from the National Center for Biotechnology Information (NCBI): cce4228 protein from *Cyanothece* sp. ATCC51142 (ACB53576), all3556 from *Anabaena* sp. PCC7120 (BAB75255), a2771 from *Synechococcus* sp. PCC7002 (ACB00745), YneI from *Samlonella typhimurium* (NP_460484), YneI from *E. coli* (WP_115463367), GabD from *E. coli* (NP_417147), GabD from *Human* (NP_001071), GabD from *A. thaliana* (NP_178062), YneI from *Bacillus subtilis* (ARW30050). Triangle indicates residues involved in cofactor preference, and pentagram indicates residues involved in enzyme catalysis.

<https://doi.org/10.1371/journal.pone.0239372.g005>

The distances between the adenosine nucleoside phosphate group of NADP⁺ and the side chain OH group and the backbone NH group of Ser157 residue were only 2.6 Å and 2.9 Å, respectively. In addition, the distances between the side chain NH₃⁺ group of Lys154 residue and the adenosine nucleoside phosphate group of NADP⁺ were in the range of 2.9–3.3 Å (Fig 6B). Once the Lys154 was mutated to Ala154 with short side chain, these interactions would be vanished. Since the Ser157 and Lys154 residues from homology model and crystal structure (PDB ID: 3VZ3) were almost overlapped, we speculated that the Ser157 and Lys154 residues from cce4228 protein would serve as determinants of cofactor preference. At the same time, this structural feature explained why the Ser157Glu and Lys154Ala mutations did not alter the binding affinity of cce4228 with SSA substrate. Meanwhile, the carboxyl group of SSA substrate was located in the vicinities of the side chains of Ser419, Trp135 and Arg139 in the crystal structure. As a comparison, the mutations of the corresponding residues in cce4228 protein of the above three residues resulted in dramatically reduced binding affinity of cce4228 protein with SSA (S2 Table in S1 File). Since Cys262 functioned as a nucleophile and Glu228 as a general base in catalytic mechanism, we could see that these two residues located near SSA and NADP⁺ (Fig 6B).

Proposed enzymatic mechanism of cce4228 protein

The enzymatic mechanisms of SSADHs were well studied previously [19, 20, 22, 25, 30–32]. The key step of proposed catalytic mechanisms of SSADHs was to form the thiohemiacetal

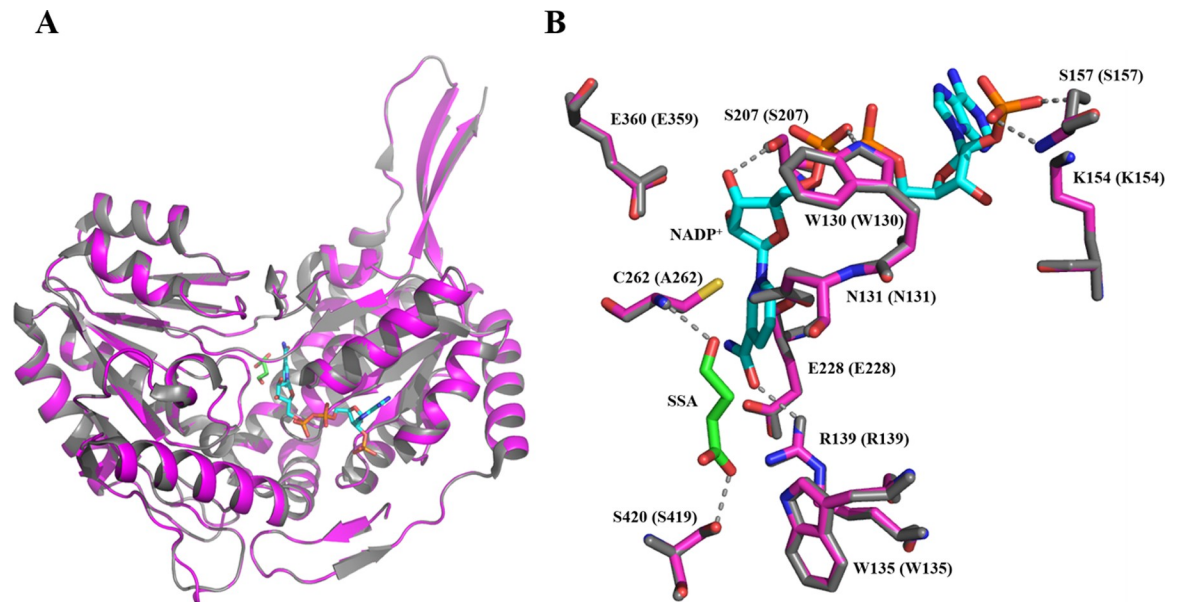


Fig 6. Structural modeling of cce4228 protein. **A.** The superposition of homology model of cce4228 protein and crystal structure of SSADH from *Synechococcus* sp. PCC7002 (PDB ID: 3VZ3), which were indicated by magenta and grey, respectively. The sticks were from the crystal structure with green (SSA) and cyan (NADP⁺) carbons. **B.** The close view of the active site. The residues with magenta and grey carbons were from homology model and crystal structure. Nitrogen, oxygen, phosphorus and sulfur atoms were colored as blue, red, orange and yellow, respectively. Residues were numbered according to the amino acid sequence of cce4228 protein. The numbers in parenthesis were from the amino acid sequence of crystal structure. The grey dashed lines indicated the possible interactions in the crystal structure. This figure was prepared by Pymol 1.503.

<https://doi.org/10.1371/journal.pone.0239372.g006>

tetrahedral intermediate. However, there were several mechanisms for this formation of key intermediate (Fig 7). First, the nucleophilic Cys residue attacked the carbonyl group of SSA directly to form this key intermediate. SSADHs from *Streptococcus pyogenes* and *Salmonella*

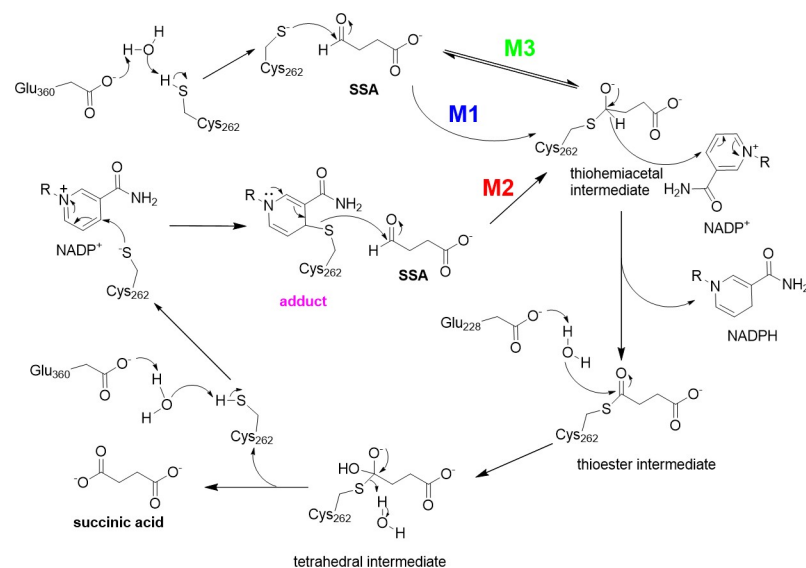


Fig 7. Proposed catalytic mechanisms for SSADHs from different sources. M1, M2 and M3 indicated the first, second and third mechanisms as stated in the text.

<https://doi.org/10.1371/journal.pone.0239372.g007>

typhimurium were the examples [22, 30]. Second, the Cys residue in the catalytic center of SSADHs from cyanobacteria such as *Synechococcus* sp. PCC7002 [20] and *Anabaena* sp. PCC7120 [25] attacked NADP⁺ cofactor first to form cofactor-cysteine adduct, which might prevent the oxidation of catalytic cysteine. Then recruited SSA was attacked by the cofactor-cysteine adduct to form the key intermediate. Third, the SSADH from *Mycobacterium tuberculosis* adopted non-rapid equilibrium random mechanism to form thiohemiacetal tetrahedral intermediate [31]. In any case, the cysteine residue in the active site functioned as nucleophilic agent. SSADHs had two protection mechanisms to prevent the single catalytic Cys from being oxidized. Firstly, the key catalytic Cys forms disulfide bonds with non-catalytic Cys residues not far away from it to protect the key catalytic Cys from oxidation. It was the case for human SSADH [33]. Secondly, the key catalytic Cys by first attacking the cofactor NADP⁺ to form an E-NADP⁺ complex to prevent its key catalytic Cys from being oxidized [20, 25]. The *cce4228* protein had only one Cys residue in the active center, therefore the redox-switch-mediated enzymatic mechanism was not appropriate for *cce4228*. To test whether *cce4228* formed an adduct with NADP⁺ cofactor in reaction solution, spectrophotometric measurements were carried out. For the *cce4228* wild-type, absorbance at the wavelength of 310~380 nm was observed clearly, which was generated by the proposed adduct [34] (Fig 8A). Since SSA substrate was not yet added into the assay solution, this absorption at 310~380 nm was not generated by NADPH, the reduced form of NADP⁺. Meanwhile, this absorption disappeared when Cys262Ala mutant substituted the *cce4228* wild-type protein (Fig 8B). Thereby, *cce4228* would adopt the second catalytic mechanism to generate the key thiohemiacetal tetrahedral intermediate. Briefly, Cys262 residue of *cce4228* would first form an adduct with NADP⁺ and then this adduct would attack SSA substrate to form the key thiohemiacetal tetrahedral intermediate, which then was converted into thioester intermediate. With the help of Glu228 as a general base, the thioester intermediate would be hydrolyzed to succinic acid and release the protein. Basically, this mechanism was consistent with that of other SSADHs from cyanobacteria [19, 20, 25].

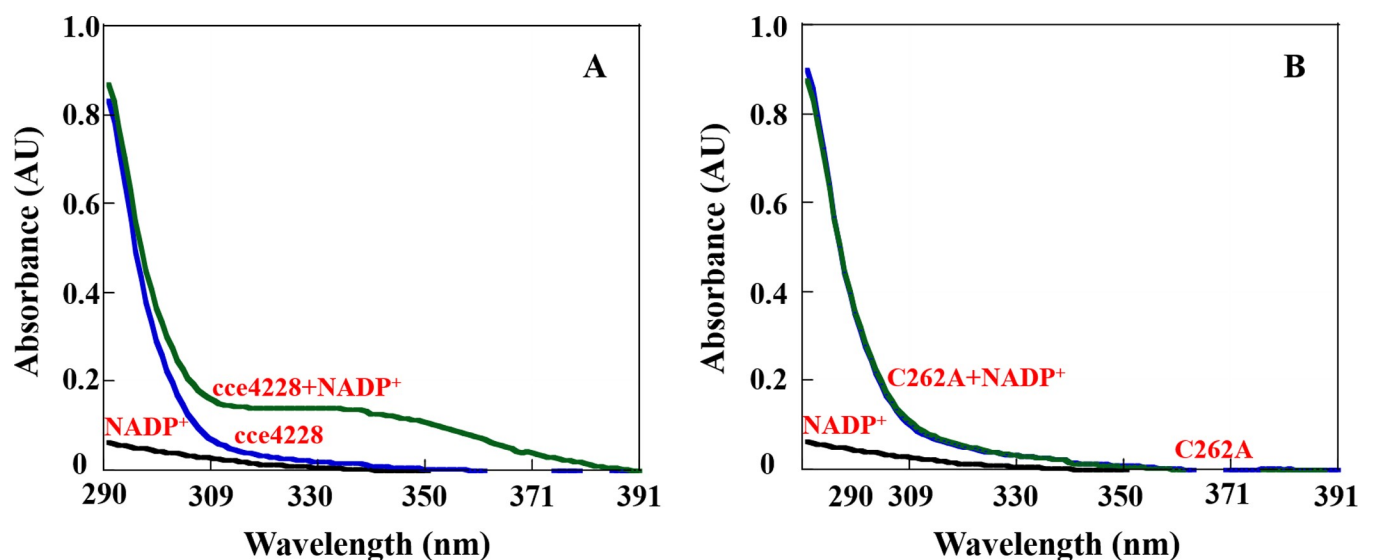


Fig 8. Spectrophotometric measurements of the cysteine-NADP⁺ adduct in solution using *cce4228* wild-type and the Cys262Ala mutant. A. The absorbance of the cysteine-NADP⁺ adduct in solution using *cce4228* wild-type. Spectra were recorded for 27 μ M *cce4228* (blue), 27 μ M NADP⁺ (black), and a mixture of 27 μ M *cce4228* and NADP⁺ (green); B. The absorbance of the cysteine-NADP⁺ adduct in solution using the Cys262Ala mutant. Spectra were recorded for 27 μ M Cys262Ala (blue), 27 μ M NADP⁺ (black), and a mixture of 27 μ M Cys262Ala and NADP⁺ (green).

<https://doi.org/10.1371/journal.pone.0239372.g008>

Conclusions

The recombinant SSADH encoded by *cce4228* gene from *Cyanothece* sp. ATCC51142 was biochemically characterized in detail. Our results demonstrated that either NAD⁺ or NADP⁺ could be used as cofactor of *cce4228* protein, although the binding affinity of NADP⁺ with *cce4228* was much higher than that of NAD⁺ with *cce4228*. Meanwhile, SSA proved to be a competitive inhibitor of *cce4228*. Kinetic and structural analysis demonstrated that the conserved Cys262 and Glu228 residues were crucial for the catalytic activity of *cce4228* protein and the Ser157 and Lys154 residues were determinants of cofactor preference. Finally, the enzymatic mechanism of *cce4228* protein was suggested on account of kinetic data and model structure.

Supporting information

S1 Raw images. Raw gel images for Fig 1.
(PDF)

S1 File.
(PDF)

Author Contributions

Conceptualization: Zhimin Li.

Data curation: Congcong Xie, Zhi-Min Li, Fumei Bai, Wei Zhang.

Formal analysis: Congcong Xie, Zhi-Min Li, Fumei Bai, Ziwei Hu.

Investigation: Congcong Xie, Zhi-Min Li, Ziwei Hu, Wei Zhang.

Project administration: Zhi-Min Li.

Supervision: Zhimin Li.

Writing – original draft: Zhimin Li.

Writing – review & editing: Zhimin Li.

References

1. Falcon LI, Magallon S, Castillo A. Dating the cyanobacterial ancestor of the chloroplast. *ISME J.* 2010; 4(6):777–83. <https://doi.org/10.1038/ismej.2010.2> PMID: 20200567.
2. Stanier R. Y, Cohen-Bazire G. Phototrophic prokaryotes: the cyanobacteria. *Annual Review of Microbiology.* 1977; 31:225–74. <https://doi.org/10.1146/annurev.mi.31.100177.001301> PMID: 410354.
3. Welsh EAL, Stockel M., Loh J., Elvitigala T., Wang T., Wollam C., et al. The genome of *Cyanothece* 51142, a unicellular diazotrophic cyanobacterium important in the marine nitrogen cycle. *Proc Natl Acad Sci USA.* 2008; 105(39):15094–9. <https://doi.org/10.1073/pnas.0805418105> PMID: 18812508; PubMed Central PMCID: PMC2567498.
4. Knoot CJ, Ungerer J, Wangikar PP, Pakrasi HB. Cyanobacteria: Promising biocatalysts for sustainable chemical production. *J Biol Chem.* 2018; 293(14):5044–52. Epub 2017/10/04. <https://doi.org/10.1074/jbc.R117.815886> PMID: 28972147; PubMed Central PMCID: PMC5892586.
5. Do Nascimento M, Battaglia ME, Sanchez Rizza L, Ambrosio R, Arruebarrena Di Palma A, Curatti L. Prospects of using biomass of N₂-fixing cyanobacteria as an organic fertilizer and soil conditioner. *Algal Research.* 2019; 43:101652. <https://doi.org/10.1016/j.algal.2019.101652>.
6. Shuyi Zhang, Bryant Donald A. The tricarboxylic acid cycle in cyanobacteria. *Science.* 2011; 334(6062):1551–3. <https://doi.org/10.1126/science.1210858> PMID: 22174252.
7. Wei Xiong, Daniel Brune, Vermaas Wim F. J. The γ -aminobutyric acid shunt contributes to closing the tricarboxylic acid cycle in *Synechocystis* sp. PCC 6803. *Molecular Microbiology.* 2014; 93(4):786–96. <https://doi.org/10.1111/mmi.12699> PMID: 24989231.

8. Green Laura S, Li Youzhong, Emerich David W, Bergersen Fraser J, Day David A. Catabolism of α -Ketoglutarate by a *sucA* Mutant of *Bradyrhizobium japonicum*: Evidence for an Alternative Tricarboxylic Acid Cycle. *Journal of bacteriology*. 2000; 182(10):2838–44. Epub 2000/04/27. <https://doi.org/10.1128/jb.182.10.2838-2844.2000> PMID: 10781553; PubMed Central PMCID: PMC101993.
9. Tian J, Bryk R, Itoh M, Suematsu M, Nathan C. Variant tricarboxylic acid cycle in *Mycobacterium tuberculosis*: identification of α -ketoglutarate decarboxylase. *Proc Natl Acad Sci USA*. 2005; 102(30):10670–5. <https://doi.org/10.1073/pnas.0501605102> PMID: 16027371; PubMed Central PMCID: PMC1180764.
10. Zhang S, Qian X, Chang S, Dismukes GC, Bryant DA. Natural and synthetic variants of the tricarboxylic acid cycle in cyanobacteria: Introduction of the GABA shunt into *Synechococcus* sp. PCC 7002. *Front Microbiol*. 2016; 7:1972. <https://doi.org/10.3389/fmicb.2016.01972> PMID: 28018308; PubMed Central PMCID: PMC5160925.
11. Donnelly MI, Cooper RA. Succinic semialdehyde dehydrogenases of *Escherichia coli*: their role in the degradation of *p*-hydroxyphenylacetate and γ -aminobutyrate. *European journal of biochemistry / FEBS*. 1981; 113(3):555–61. Epub 1981/01/01. <https://doi.org/10.1111/j.1432-1033.1981.tb05098.x> PMID: 7011797.
12. Malaspina P, Rouillet JB, Pearl PL, Ainslie GR, Vogel KR, Gibson KM. Succinic semialdehyde dehydrogenase deficiency (SSADHD): Pathophysiological complexity and multifactorial trait associations in a rare monogenic disorder of GABA metabolism. *Neurochem Int*. 2016; 99:72–84. Epub 2016/06/18. <https://doi.org/10.1016/j.neuint.2016.06.009> PMID: 27311541; PubMed Central PMCID: PMC5028283.
13. Lin CY, Weng WC, Lee WT. A novel mutation of *ALDH5A1* gene associated with succinic semialdehyde dehydrogenase deficiency. *J Child Neurol*. 2015; 30(4):486–9. Epub 2014/09/24. <https://doi.org/10.1177/0883073814544365> PMID: 25246302.
14. Kyung-Jin Kim, Pearl Phillip L, Kimmo Jensen, Carter Snead O., Patrizia Malaspina, Cornelis Jakobs, et al. Succinic semialdehyde dehydrogenase: biochemical-molecular-clinical disease mechanisms, redox regulation, and functional significance. *Antioxidants & Redox Signaling*. 2011; 15(3):691–718. <https://doi.org/10.1089/ars.2010.3470> PMID: 20973619; PubMed Central PMCID: PMC3125545.
15. Koichi Toyokura, Keiro Watanabe, Akira Oiwa, Miyako Kusano, Toshiaki Tameshige, Kiyoshi Tate-matsu, et al. Succinic Semialdehyde Dehydrogenase is Involved in the Robust Patterning of Arabidopsis Leaves along the Adaxial-Abaxial Axis. *Plant & Cell Physiology*. 2011; 52(8):1340–53. <https://doi.org/10.1093/pcp/pcr079> PMID: 21690177.
16. Bouche N, Fait A, Bouchez D, Moller SG, Fromm H. Mitochondrial succinic-semialdehyde dehydrogenase of the γ -aminobutyrate shunt is required to restrict levels of reactive oxygen intermediates in plants. *Proc Natl Acad Sci USA*. 2003; 100(11):6843–8. <https://doi.org/10.1073/pnas.1037532100> PMID: 12740438; PubMed Central PMCID: PMC164534.
17. Schneider Barbara L, Reitzer Larry. Pathway and enzyme redundancy in putrescine catabolism in *Escherichia coli*. *Journal of bacteriology*. 2012; 194(15):4080–8. <https://doi.org/10.1128/JB.05063-11> PMID: 22636776; PubMed Central PMCID: PMC3416515.
18. Murphy TCA, Gibson Venkataraman, Michael Picklo K. Sr, Matthew J. Oxidation of 4-hydroxy-2-nonenal by succinic semialdehyde dehydrogenase (*ALDH5A*). *J Neurochem*. 2003; 86(2):298–305. <https://doi.org/10.1046/j.1471-4159.2003.01839.x> PMID: 12871571
19. Yuan Z, Yin B, Wei D, Yuan YR. Structural basis for cofactor and substrate selection by cyanobacterium succinic semialdehyde dehydrogenase. *J Struct Bio*. 2013; 182(2):125–35. <https://doi.org/10.1016/j.jsb.2013.03.001> PMID: 23500184.
20. Jinseo Park, Sangkee Rhee. Structural basis for a cofactor-dependent oxidation protection and catalysis of cyanobacterial succinic semialdehyde dehydrogenase. *The Journal of biological chemistry*. 2013; 288(22):15760–70. <https://doi.org/10.1074/jbc.M113.460428> PMID: 23589281; PubMed Central PMCID: PMC3668734.
21. Park SA, Park YS, Lee KS. Kinetic characterization and molecular modeling of NAD(P)(+)-dependent succinic semialdehyde dehydrogenase from *Bacillus subtilis* as an ortholog *YneI*. *J Microbiol Biotechnol*. 2014; 24(7):954–8. <https://doi.org/10.4014/jmb.1402.02054> PMID: 24809290.
22. Zheng H, Beliaevsky A, Tchigvintsev A, Brunzelle JS, Brown G, Flick R, et al. Structure and activity of the NAD(P)+-dependent succinate semialdehyde dehydrogenase *YneI* from *Salmonella typhimurium*. *Proteins*. 2013; 81(6):1031–41. Epub 2012/12/12. <https://doi.org/10.1002/prot.24227> PMID: 23229889.
23. Fuhrer T, Chen L, Sauer U, Vitkup D. Computational prediction and experimental verification of the gene encoding the NAD+/NADP+-dependent succinate semialdehyde dehydrogenase in *Escherichia coli*. *J Bacteriol*. 2007; 189(22):8073–8. Epub 2007/09/18. <https://doi.org/10.1128/JB.01027-07> PMID: 17873044; PubMed Central PMCID: PMC2168661.
24. Jang EH, Park SA, Chi YM, Lee KS. Kinetic and structural characterization for cofactor preference of succinic semialdehyde dehydrogenase from *Streptococcus pyogenes*. *Mol Cells*. 2014; 37(10):719–26.

- Epub 2014/09/27. <https://doi.org/10.14348/molcells.2014.0162> PMID: 25256219; PubMed Central PMCID: PMC4213762.
25. Xiaoqin Wang, Chongde Lai, Guofeng Lei, Fei Wang, Haozhi Long, Xiaoyu Wu, et al. Kinetic characterization and structural modeling of an NADP(+)-dependent succinic semialdehyde dehydrogenase from *Anabaena* sp. PCC7120. *International Journal of Biological Macromolecules*. 2018; 108:615–24. <https://doi.org/10.1016/j.ijbiomac.2017.12.059> PMID: 29242124.
 26. Xie C, Li Z-M, Wang X, Lei G, Zhang W, Li Z. Expression and characterization of succinic semialdehyde dehydrogenase from *Cyanothece* sp. ATCC51142. *Microbiology China*. 2019; 46(11):2933–43. <https://doi.org/10.13344/j.microbiol.china.181034>
 27. Biasini M, Bienert S, Waterhouse A, Arnold K, Studer G, Schmidt T, et al. SWISS-MODEL: modelling protein tertiary and quaternary structure using evolutionary information. *Nucleic Acids Res*. 2014; 42 (Web Server issue):W252–8. <https://doi.org/10.1093/nar/gku340> PMID: 24782522; PubMed Central PMCID: PMC4086089.
 28. Rigsby RE, Parker AB. Using the PyMOL application to reinforce visual understanding of protein structure. *Biochemistry and Molecular Biology Education*. 2016; 44(5):433–7. <https://doi.org/10.1002/bmb.20966> PMID: 27241834
 29. Vanlerberghe GC, Yip JY, Parsons HL. In Organello and in Vivo Evidence of the Importance of the Regulatory Sulfhydryl/Disulfide System and Pyruvate for Alternative Oxidase Activity in Tobacco. *Plant Physiol*. 1999; 121(3):793–803. Epub 1999/11/11. <https://doi.org/10.1104/pp.121.3.793> PMID: 10557227; PubMed Central PMCID: PMC59441.
 30. Anna-Kaisa Niemi a Candida Brownb, Moorec Tereza, Ennsa Gregory M., Cowanc Tina M.. Evidence of redox imbalance in a patient with succinic semialdehyde dehydrogenase deficiency. *Molecular genetics and metabolism reports*. 2014. <https://doi.org/10.1016/j.ymgmr.2014.02.005> PMID: 27896081
 31. de Carvalho Luiz Pedro S, Yan Ling, Chun Shen, David Warren J., Rhee Kyu Y. On the chemical mechanism of succinic semialdehyde dehydrogenase (GabD1) from *Mycobacterium tuberculosis*. *Arch Biochem Biophys*. 2011; 509(1):90–9. <https://doi.org/10.1016/j.abb.2011.01.023> PMID: 21303655 PubMed PMID: ISI:000289928800012.
 32. Yeon-Gil Kim, Sujin Lee, Oh-Sin Kwon, So-Young Park, Su-Jin Lee, Bum-Joon Park, et al. Redox-switch modulation of human SSADH by dynamic catalytic loop. *The EMBO Journal*. 2009; 28(7):959–68. <https://doi.org/10.1038/emboj.2009.40> PMID: 19300440; PubMed Central PMCID: PMC2670868.
 33. Kim YG, Lee S, Kwon OS, Park SY, Lee SJ, Park BJ, et al. Redox-switch modulation of human SSADH by dynamic catalytic loop. *EMBO J*. 2009; 28(7):959–68. <https://doi.org/10.1038/emboj.2009.40> PMID: 19300440; PubMed Central PMCID: PMC2670868.
 34. Tsybovsky Y, Donato H, Krupenko NI, Davies C, Krupenko SA. Crystal structures of the carboxyl terminal domain of rat 10-formyltetrahydrofolate dehydrogenase: implications for the catalytic mechanism of aldehyde dehydrogenases. *Biochemistry*. 2007; 46(11):2917–29. Epub 2007/02/17. <https://doi.org/10.1021/bi0619573> PMID: 17302434.